

RECEIVED
CENTRAL FAX CENTER

JAN 26 2006

BEST AVAILABLE COPY

EXHIBIT A

First results from epitaxial GaN detectors

W. Cunningham¹, M. Rahman¹, J. Vaitkus², E. Gaubas², P.J. Sellin³, D. Hoxley³, A. Lohstroh³, A. Simon⁴,

¹Department of Physics, University of Glasgow

²Institute of Materials Science and Applied Research, Vilnius University

³Radiation Imaging Group, Department of Physics, University of Surrey

⁴Surrey Centre for Ion Beam Applications, University of Surrey

p.sellin@surrey.ac.uk

www.ph.surrey.ac.uk/cnrrp/imaging

Introduction

- ❑ An initial characterisation has been made of epitaxial GaN detectors - a material of potential interest for X-ray imaging and charged particle detection
- ❑ Si epitaxial GaN of 2 μm thickness has been studied with alpha particles:
 - \Rightarrow expect good charge collection efficiency
- ❑ CV analysis used to measure carrier concentration and material purity
- ❑ material uniformity was imaged using a focussed alpha particle beam with a 1 μm spatial resolution
- ❑ the effect of radiation damage was also investigated by irradiating devices with 600 Mrad of photons and $5 \times 10^{14} \text{ cm}^{-2}$ of neutrons

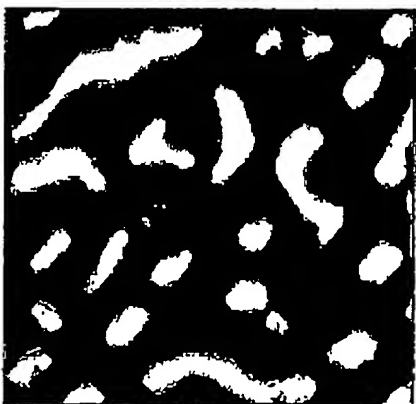
Properties of GaN

GaN is slightly n-type, with semi-insulating (SI) material available in thin layers:

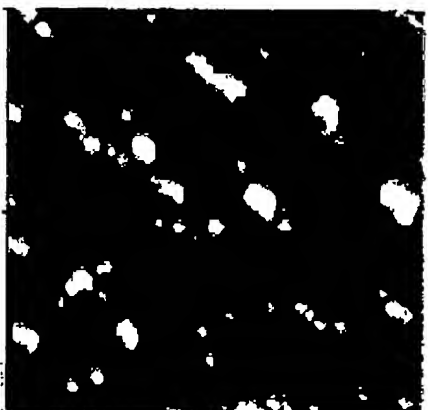
Cubic GaN	
Z (fraction by weight)	31 (0.83), 7 (0.17)
Density	6.15 g cm ⁻³
Band gap (eV)	3.2 eV (300K) 3.0 eV (0K)
Dielectric constant	8.9
Electron mobility μ_e	~600 cm ² /Vs
Hole mobility μ_h	200-400 cm ² /Vs
Saturated drift velocity v_e	2.5 x 10 ⁷ cm/s

Epitaxial GaN tends to show a highly defective, ordered polycrystalline growth with a columnar structure - on a nanometre length scale.

D. Huano et al. Journal of Vacuum Science and Technology B 20 (2002) 2256-2264



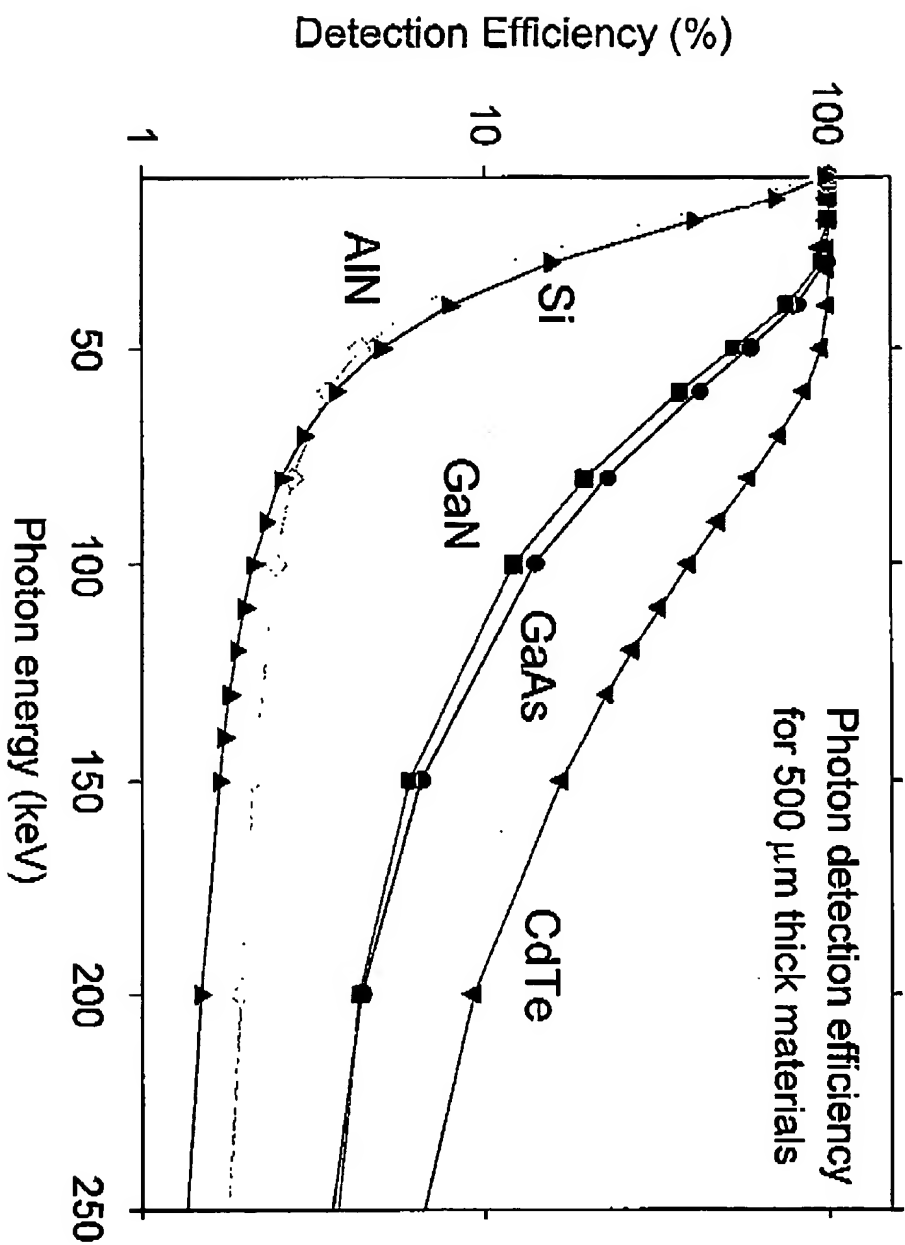
AFM images of epitaxial GaN samples. Image size is 2 μ m x 2 μ m



Paul Sellin, Radiation Imaging Group

Photon Detection Efficiency for GaN

Atomic numbers of 31 and 7 provide good photoelectric absorption cross-sections:



Growth of epitaxial GaN

Thin epitaxial GaN layers are grown by metal organic chemical

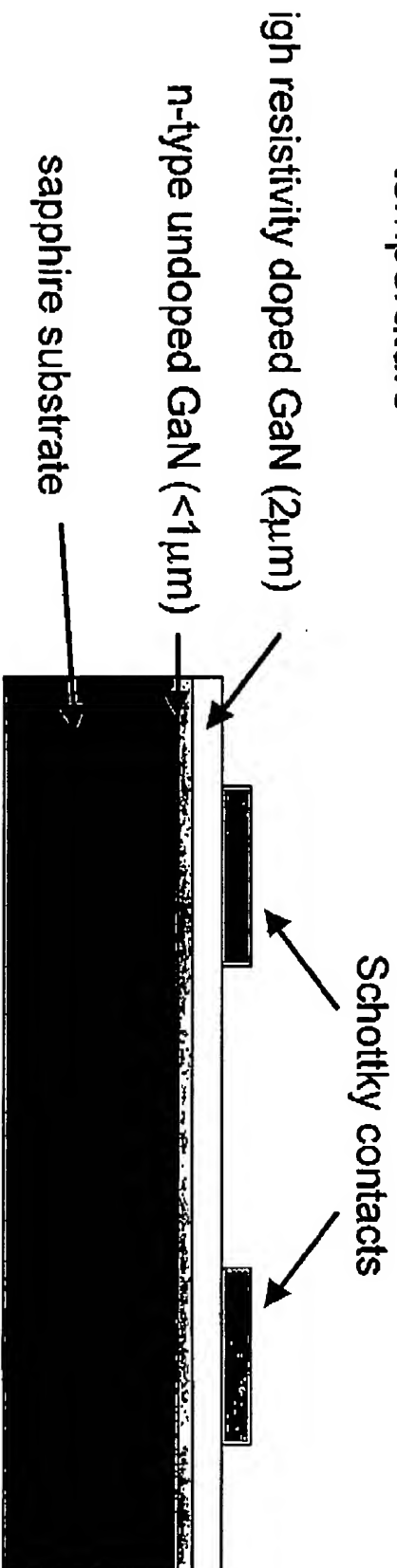
vapour deposition (MOCVD) - University of Tokushima, Japan

Growth process uses sapphire as a substrate, with an n-type
conducting GaN buffer layer

High purity semi-insulating (SI) GaN layer is grown on top of the
buffer layer

Typical SI GaN layer thickness is $2\text{ }\mu\text{m}$

Mobility and carrier density can be optimised by varying growth
temperature



T. Wang et al, Applied Physics Letters 76 (2000) 2220-2222

Epitaxial GaN detectors



The GaN test device was mounted onto ceramic and characterised with alpha particles.

2 additional devices were irradiated for radiation hardness studies - for particle physics applications:

- ⇒ 600 MRad of X-rays
- ⇒ $5 \times 10^{14} \text{ cm}^{-2}$ of 1 MeV neutrons

Bulk GaN crystals

SI GaN crystals have been under development for several years, particularly at Warsaw:

Grown in liquid Ga with N_2 over pressure:
20 kbar and 1700 °C

Undoped

\Rightarrow n-type at 10^{19} cm^{-3} , $p \sim 10^{-3}$ - $10^{-2} \Omega\text{cm}$

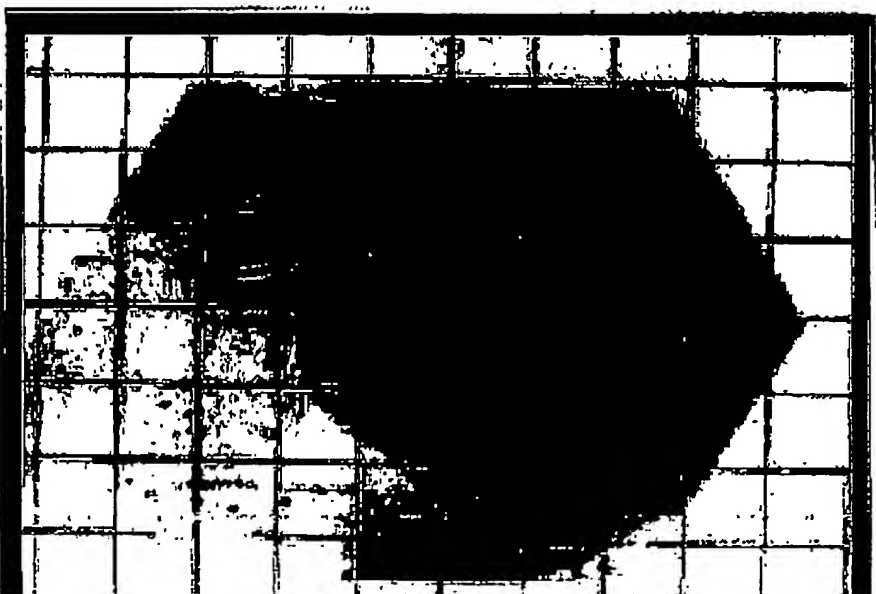
Grown with 0.5% Mg

\Rightarrow semi insulating, $p \sim 10^4$ - $10^6 \Omega\text{cm}$

SI material has residual concentration of $\sim 10^{16} \text{ cm}^{-3}$ - very poor charge transport

S. Porowski, J Cryst Growth 189/190 (1998) 153-158

JnS Department of Physics
University of Surrey

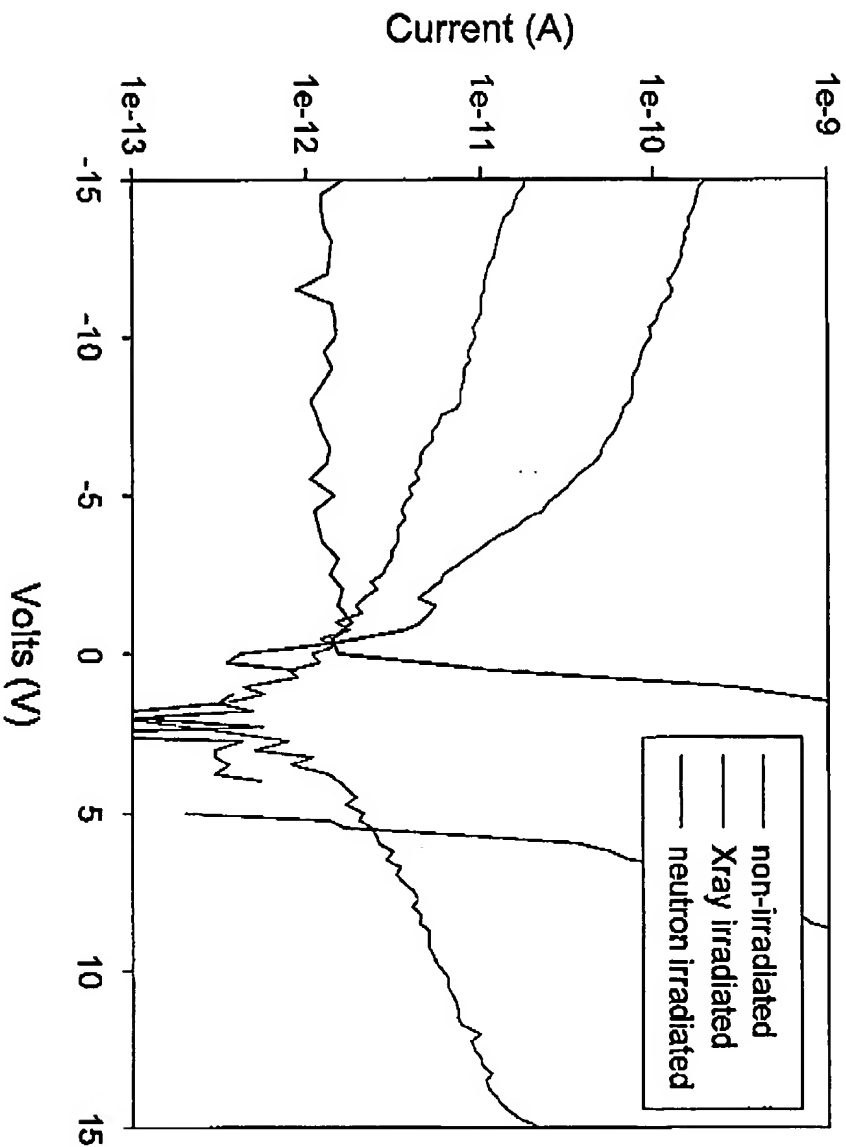


GaN single crystal
(1mm grid)

Paul Sellin, Radiation Imaging Group

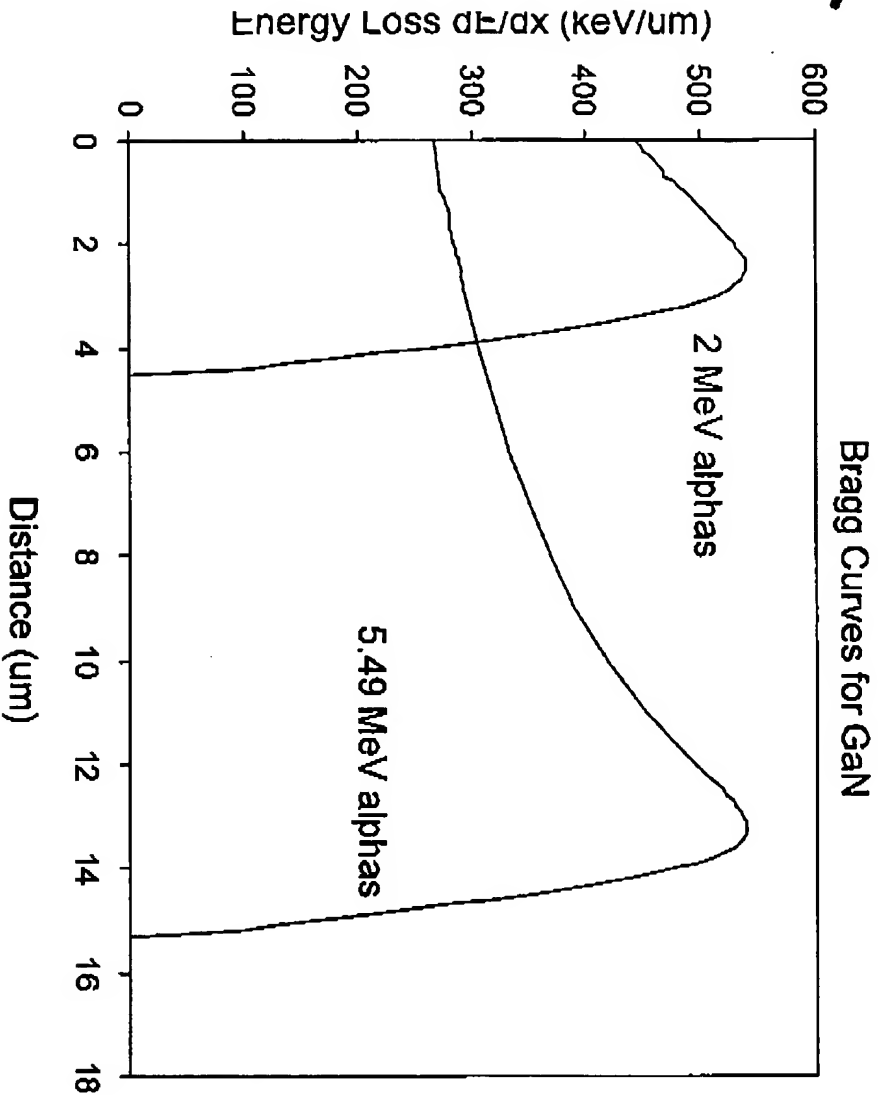
IV characteristics

IV data on epitaxial device shows good diode characteristics from Schottky contact. Reverse-bias current $\sim 10^{-12}$ A at -15 V ($J = 6 \times 10^{-11}$ A/cm²)



Bragg curves in GaN

Alpha particle range is much greater than 2 μm active thickness of GaN layer:



Energy deposited by
alpha particles in 2 mm of
GaN estimated from
Bragg curves (SRIM):

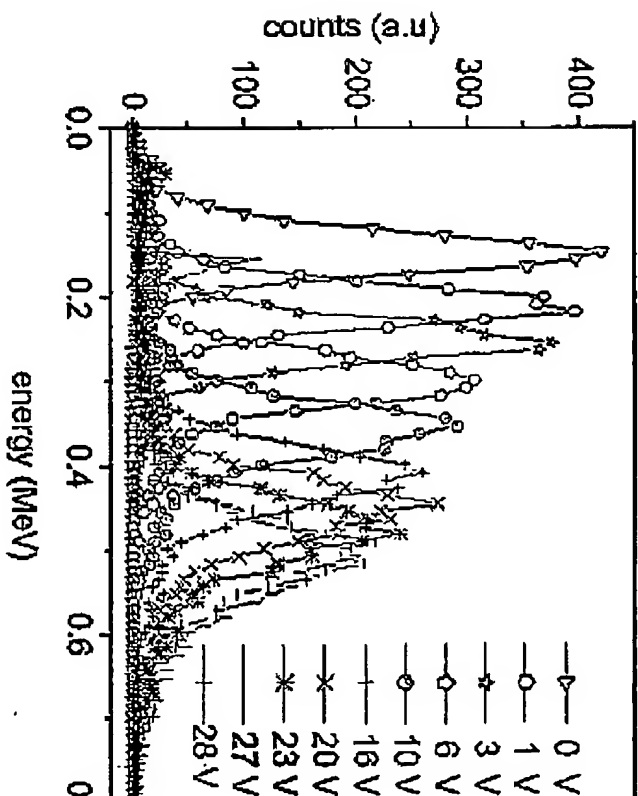
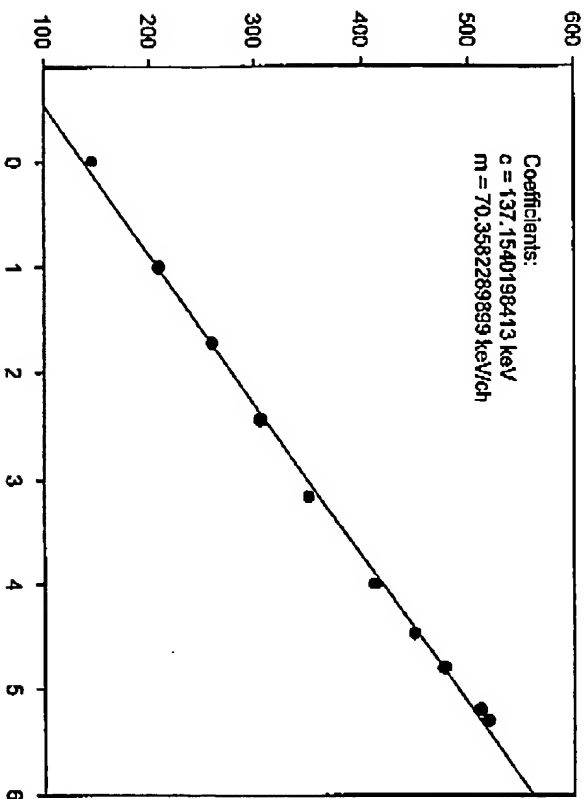
2 MeV alpha: 949 keV

5.49 MeV alpha: 553 keV

Alpha particle spectra

Room temperature alpha particle spectra:

⇒ systematic increase in measured energy as a function of bias voltage, as field strength increases
 ⇒ no evidence for charge trapping in this thin material



Plotting alpha peak centroid vs $V^{1/2}$:

⇒ extrapolate to deposited energy in $2\mu\text{m}$ of 553 keV
 ⇒ shows full charge extraction from layer at $V=35\text{V}$

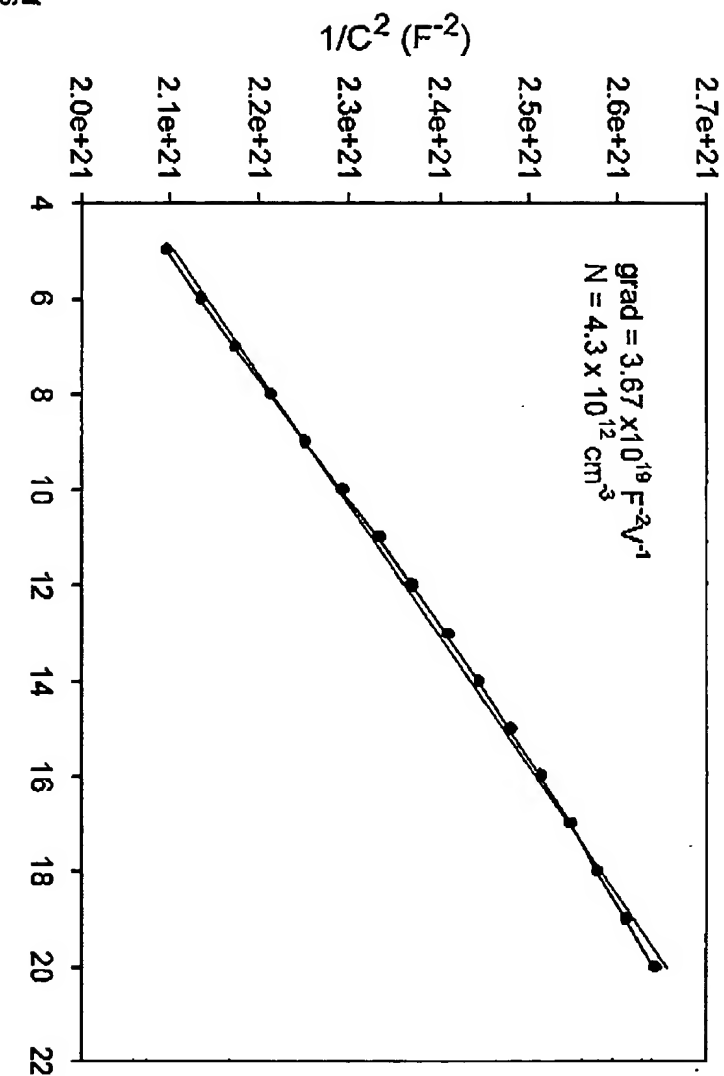
Paul Sellin, Radiation Imaging Group

CV analysis of GaN

The net impurity concentration N_D is calculated from room temperature CV measurements using

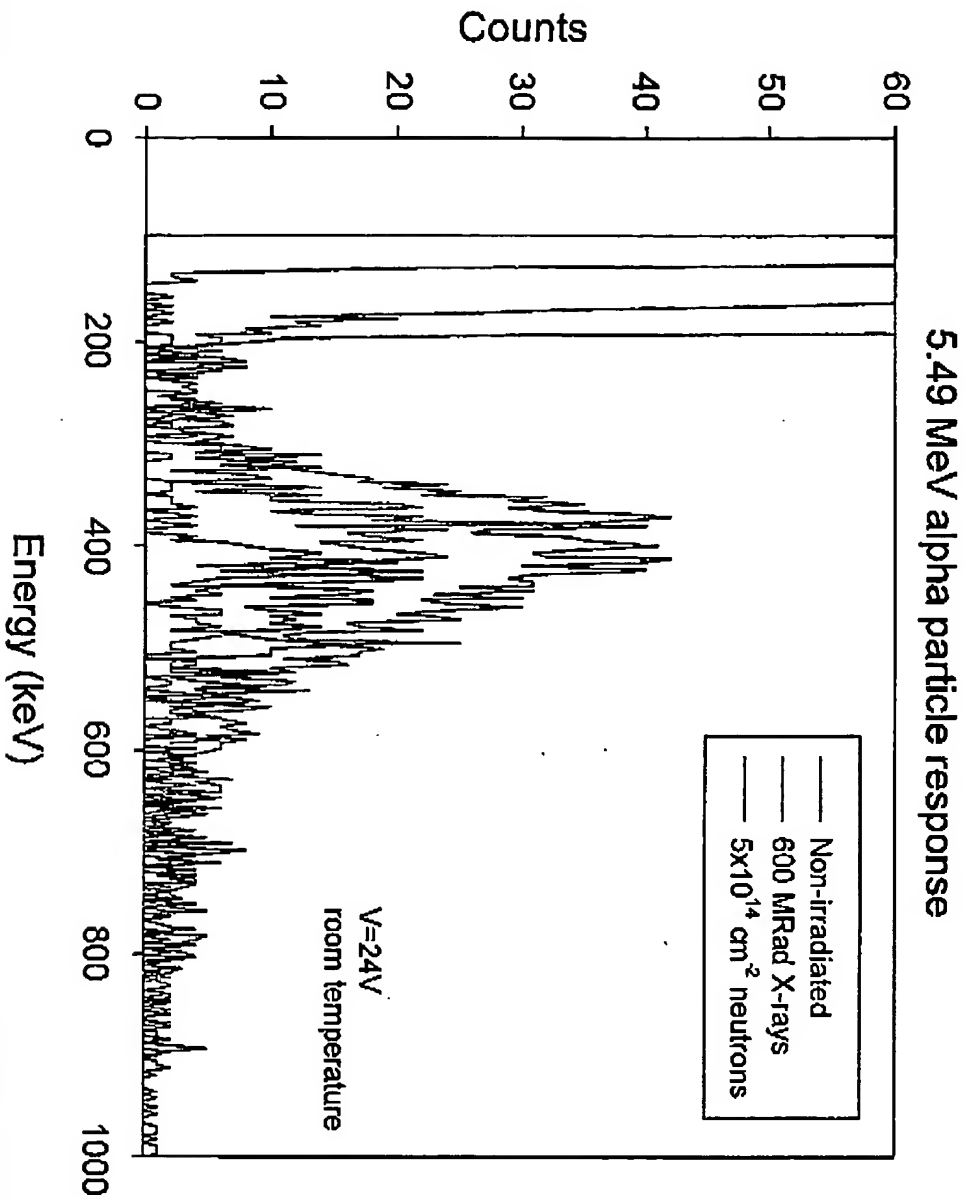
$$N_D = \frac{2}{q\epsilon_0\epsilon_R A^2} \frac{d(1/C^2)/dV}{}$$

For 1.5 mm diameter contact pads, $N_D = 1 \times 10^{13} \text{ cm}^{-3}$ - good quality material

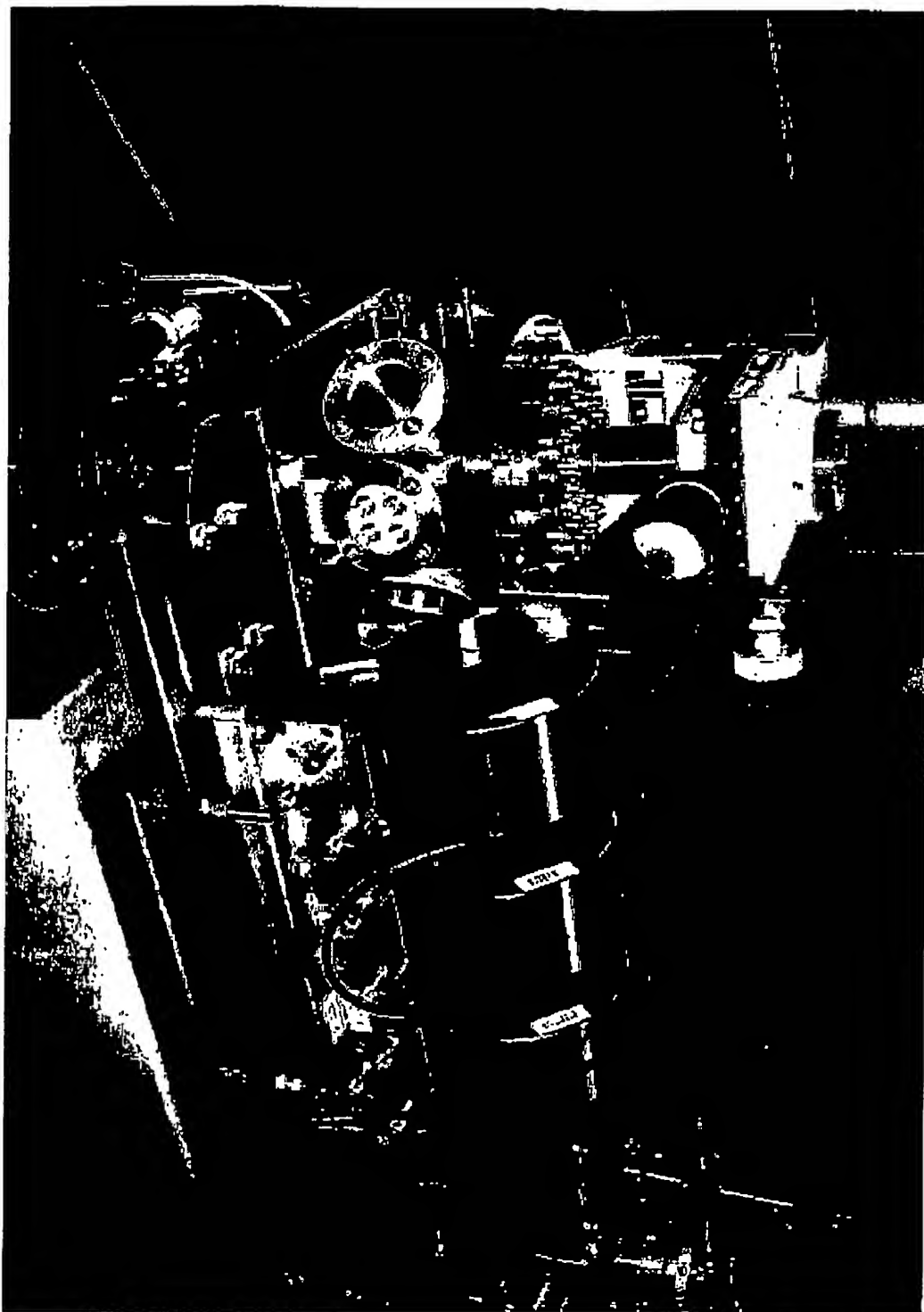


Alpha particle response of irradiated devices

2 devices were irradiated to investigate radiation hardness - with
600 MRad X-rays and 5×10^{14} cm⁻² neutrons:



The Surrey Ion Beam Microprobe

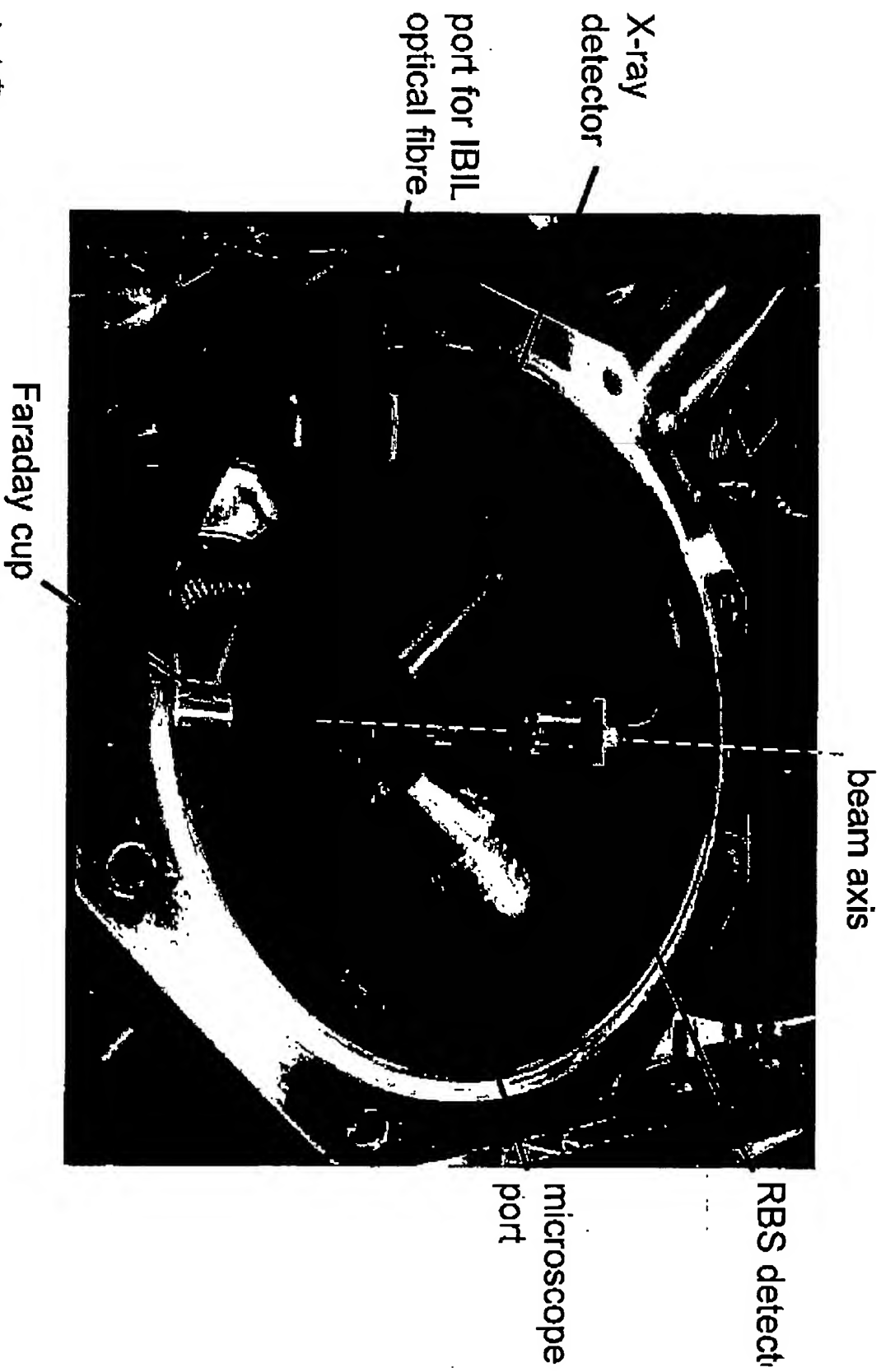


JnIS
Department of Physics
University of Surrey

2 MeV alpha particles, with event rates on the
sample of 100 Hz - 1 KHz

Paul Sellin, Radiation Imaging Group

The microbeam chamber



DNIS Department of Physics
University of Surrey

Paul Sellin, Radiation Imaging Group

Ion Beam Induced Charge (IBIC) measurements

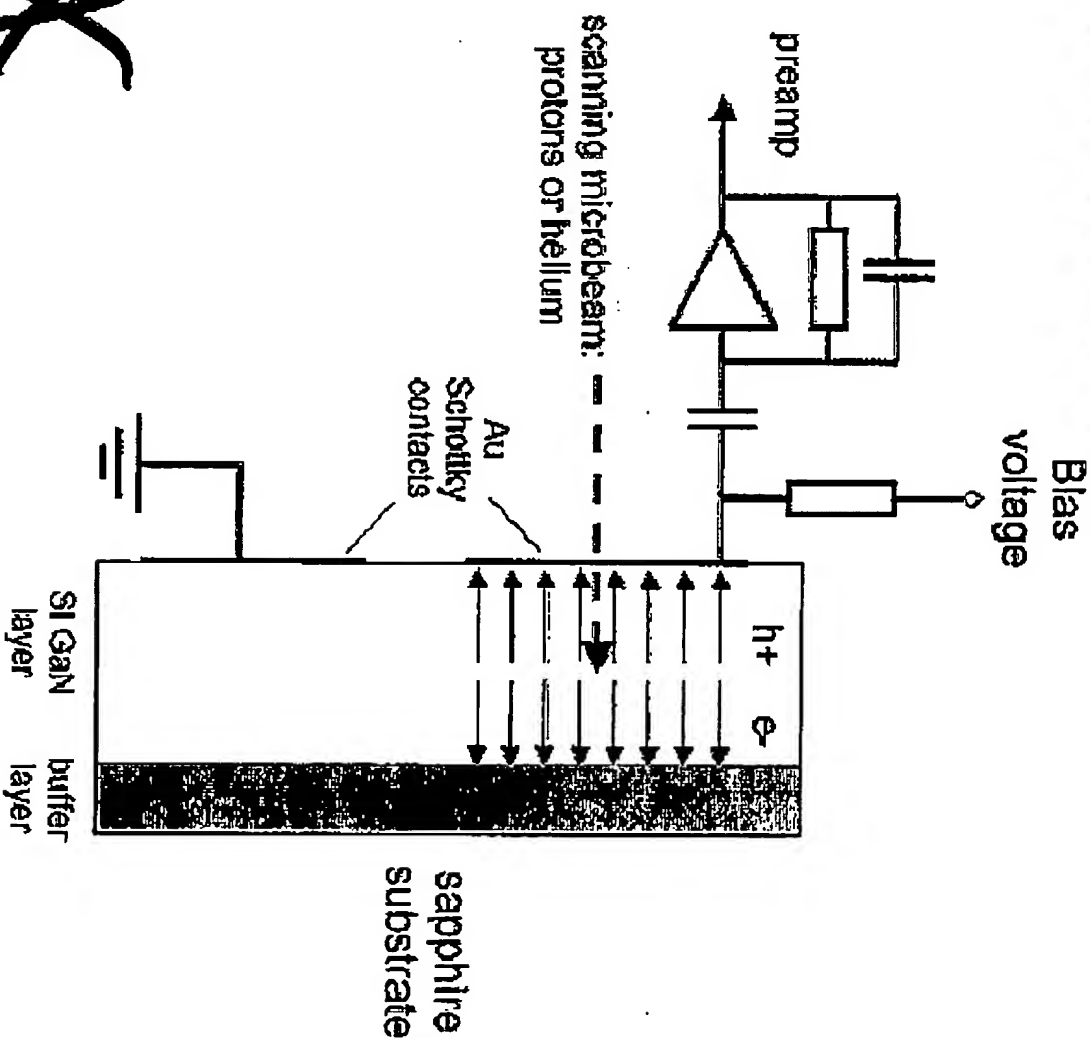
Ion Beam Induced Charge (IBIC) data provides:

- high spatial resolution imaging of charge signal uniformity
- single event detection (~1 KHz event rate on sample)
- true bulk measurement

Ion beam is incident orthogonal to one of the electrodes:

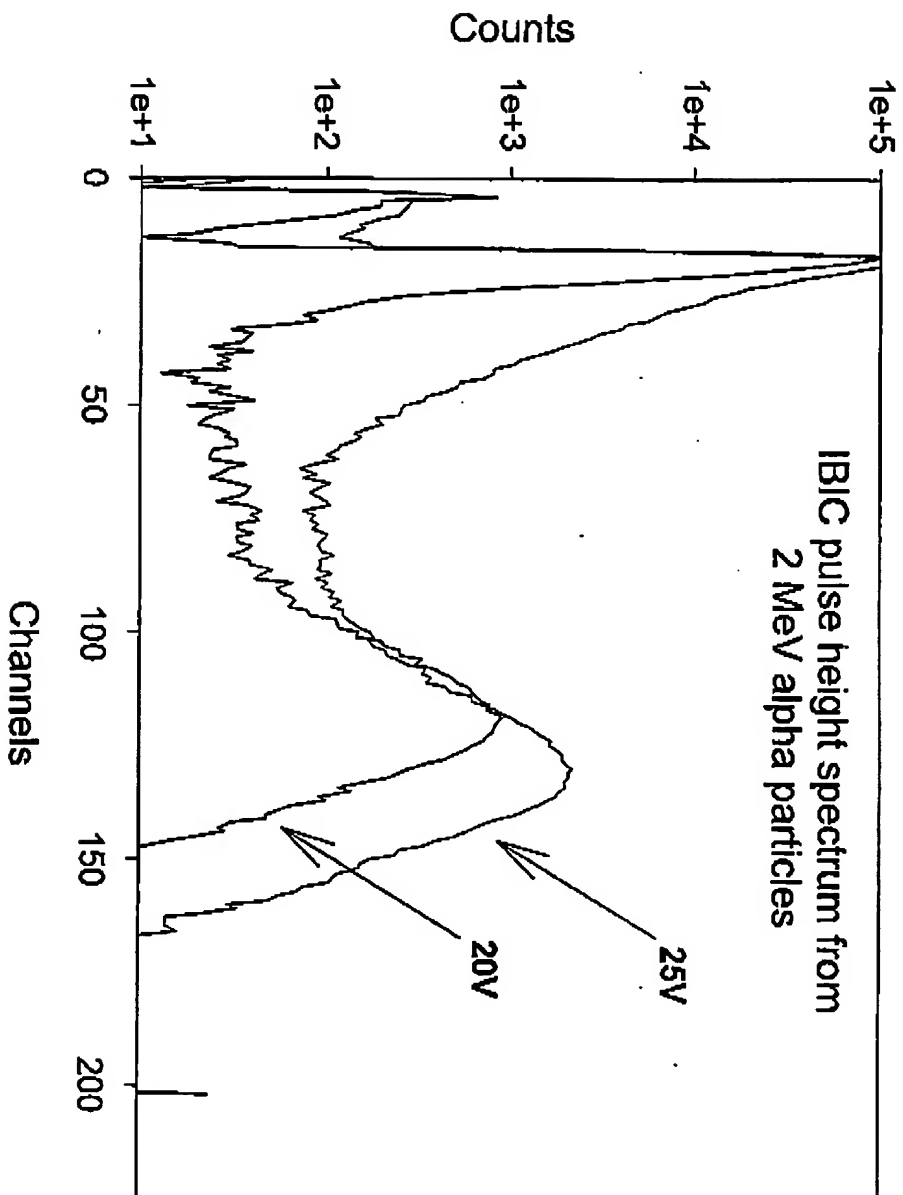
- charge drift through the Si GaN layer to the conducting buffer layer
- alpha beam cannot pass through silver DAG

JNIS Department of Physics
University of Surrey



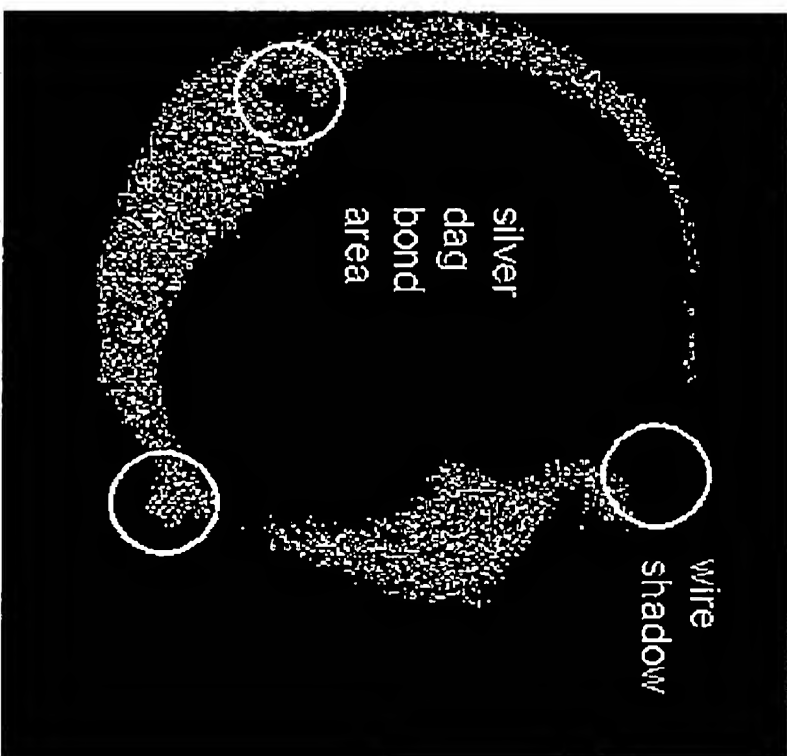
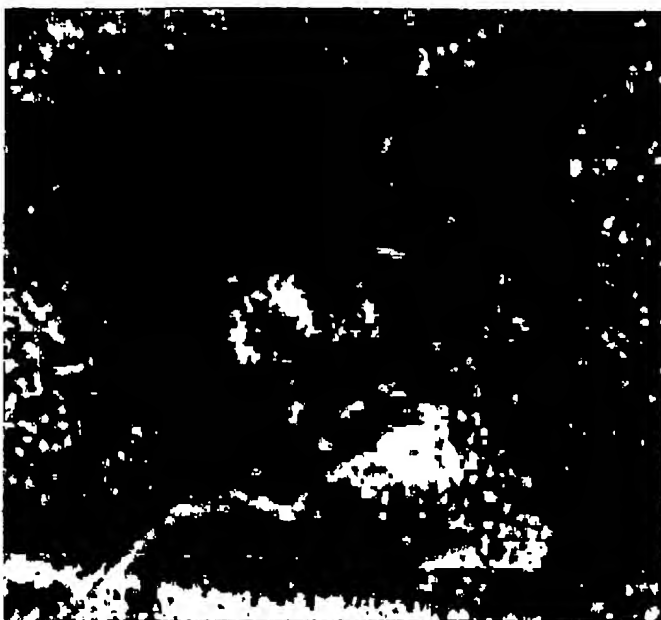
Alpha IBIC spectra from GaN

SRIM estimate of energy loss in 2 μm layer = 950 keV
Saturation of peak centroid at $V=25\text{V}$



GaN IBIC images

GaN IBIC images show charge transport only under contact pad
Excellent uniformity of signal with no field enhancement at edges
Contact is mainly obscured by silver dag bond wire



Conclusions

We have carried out a preliminary characterisation of three epitaxial Si-GaN detectors:

- ☐ High purity Si GaN detector of 2 μm thickness shows good alpha particle response
- ☐ Gold Schottky contacts show good diode behaviour - reverse bias leakage current is $\sim 10^{-12}$ A at -15V ($J = 6 \times 10^{-11}$ A/cm²)
- ☐ CV analysis gives a carrier concentration of 1×10^{13} cm⁻³
- ☐ initial IBIC imaging shows excellent material uniformity and $\sim 100\%$ CCE in very thin layers
- ☐ further measurements are required with thicker epitaxial layers, whilst maintaining $\sim 10^{13}$ cm⁻³ carrier concentration

CONTAMINATION OF NAKHLA BY TERRESTRIAL MICROORGANISMS. J.K.W Toporski¹, A. Steele², D. Stapleton³ and D.T. Goddard⁴, ¹ *School of Earth, Environmental and Physical Sciences, University of Portsmouth, Burnaby Building, Portsmouth PO1 3QL, UK, jan.toporski@port.ac.uk;* ² *Mail code SN, NASA, Lyndon. B. Johnson Space Center, Houston, Texas, 77058, USA;* ³ *BNFL, Springfields Site, Preston, UK;* ⁴ *Fujitsu Europe Ltd, Uxbridge, UK.*

Introduction Ever since meteorites have been known to come from an extraterrestrial origin people have speculated as to whether they could contain evidence of life. This was again exemplified by the claims of McKay et al. [1]. In each case the scientific community as a whole has regarded such claims of life with a certain amount of incredulity and upon the furnishing of evidence of terrestrial contamination, has dismissed the claims with alacrity. However, the actual sources of contamination within meteorites and the mechanisms of entry of such contamination still remain poorly understood. With the discovery of a probable terrestrial bacterial contaminant on ALH84001, the argument of contamination has taken another turn [2]. The findings of several researchers into the organic material within this meteorite concluded that contamination was present but then presented unfeasible arguments as to its origin from Antarctic ice [3, 4]. All the groups failed to detect an organism living on this meteorite. Not a good omen for future exploration of our solar system. With this in mind when the allocation of Nakhla became available it seemed sensible to screen this meteorite for contamination by terrestrial microorganisms.

Materials and Methods With the aim to detect possible terrestrial microbial contaminants, Scanning Electron Microscopy (SEM) investigations were carried out on samples from Nakhla. Our allocation consisted of chips taken from four sites across the meteorite, none of which was adjacent to macroscopic fractures. These samples were numbered I to IV. Sample I contained fusion crust, sample II was taken from just underneath the fusion crust, sample III originated from the interior of the meteorite, sample IV was from near the center of the meteorite. No visible fractures were observed in the meteorite.

Small chips were removed from each sample in sterile conditions under laminar flow. All instruments were presterilized by flaming or autoclaving. Chips were then visually characterised and the majority of each sample area allocation retained for culturing and organic surface analysis techniques. Small fractions of each sample chosen for SEM investigation were mounted onto aluminium stubs using carbon tape. To increase sample conductivity silver dag was sparingly used to connect the base of the samples with the stub. The samples were AuPd-coated for 45 seconds

after allowing 30 hours drying time for the silver dag under contamination free conditions. All samples were imaged with a JEOL SM 6100 fitted with a light element Energy Dispersive X-Ray Analyser (EDX).

Results The results presented in this abstract are from extensive imaging studies of chips from all four sample areas. Culturing experiments have begun but the data are not available at the time of writing this abstract. Figure 1 shows the presence of a hyphae forming organism on sample I (fusion crust). The hyphae appear to be growing from a 2 µm diameter spherical structure, which strongly resembles a fungal spore. Figure 2 shows the terminal end of a single hyphae on the fusion crust. The hyphal structure appears to be disrupted and flattened. This is not surprising, as these samples received none of the pre-treatment normally required for biological imaging. Small 100 nm circular objects are seen both associated and removed from the hyphal terminus.

Figures 3 and 4 are related to sampled IV. Figure 3 again shows the presence of hyphal filaments originating from an apparent spore-like structure. The surface appears to be covered with a thin film with the underlying mineral edges becoming indistinct. Figure 4 shows a hyphal structure appearing through the matrix of the meteorite and terminating after approximately 15 µm (terminus out of sight of the bottom of the image). Again, evidence can be seen of a coating, blurring the edges of the mineral phases, most notably in the bottom left-hand part of the image. EDX-analysis of the apparent coating showed consistently the presence of a carbon peak, which is not seen on the apparently uncoated mineral surfaces.

No evidence of any organisms was found on samples II and III although due to the heterogeneity of occurrence of the contaminant they may be present [5].

Discussion Figures 1 and 2 show the presence of probable fungal contaminants on the surface of the fusion crust. The 100 nm spheres shown in figure 2 have either formed mineralogically or from the dehydration of the hydrated polymeric substances normally secreted by microorganisms. Although these are the most plausible explanations, labeling these structures nanobacteria would require further collaborative evidence from culturing studies.

CONTAMINATION OF NAKHLA BY TERRESTRIAL MICROORGANISMS: J.K.W. Toporski et al.

Figures 3 and 4 appear to show that this fungal contaminant has managed to infiltrate to the center of the meteorite. Even though no visible fractures could be observed, small cracks and fissures must exist to allowing the organism to infiltrate. These need be no larger than the diameter of the fungal hyphae (approximately 1 μm).

The presence of large areas of a carbon rich film (fig. 3 and 4) is puzzling as the hyphal structures do not appear to be part of the film, rather they seem to sit on top of it. The appearance of the coating would neither be expected if, as it appears, it was a product of microbial activity, as any bacterial coating would dehydrate to strand-like appearance [6]. Therefore, it could represent deposits of a type of insoluble organic material indigenous to the meteorite and maybe providing a nutrient source for the fungal colonies inhabiting this meteorite.

From this study we conclude that all organic analysis conducted on this new Nakhla allocation should be undertaken with reservations. It is our contention that adequate screening methods be developed to ensure the accurate analysis of any indigenous organic material. However, as these organisms are living on extraterrestrial material they probably provide one of the best tools to study how life may exist elsewhere in the solar system.

References [1] McKay D.S. et al. (1996) *Science*, 273, 924. [2] Steele A. et al. (1999): Imaging an unknown organism on ALH84001. *Abstracts to the 30th Lunar and Planetary Science Conference 1999*. [3] Bada J.L. et al. (1998) *Science*, 279, 362-365. [4] Jull A.J.T. et al. (1998) *Science*, 279, 365-369. [5] Steele A. et al. (1998) *Meteoritics & Planetary Science*, 33, 4. [6] Steele A. (1996) PhD Thesis, University of Portsmouth, Portsmouth, UK.

Acknowledgements Monica Grady, Mike Summers, Bob Loveridge.

Fig. 1. SEM image of a hyphae forming organism on the fusion crust of sample I.

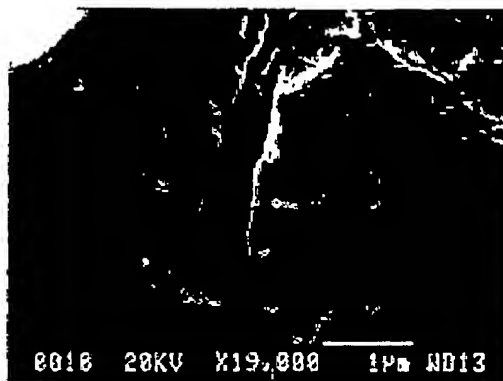


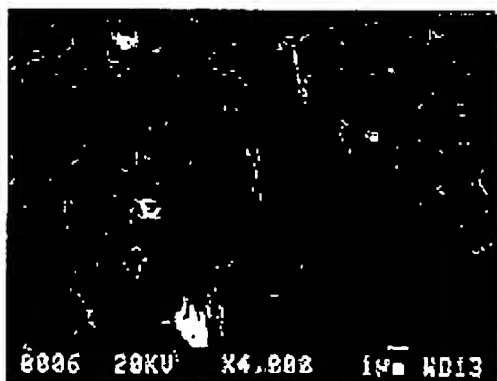
Fig. 2. SEM image showing the terminal end of a single hyphae with small spheres on the fusion crust.



Fig. 3. Hyphal filaments originating from an apparent spore-like structure and coating film on sample IV.



Fig. 4. Single filamentous hyphae structure on sample IV; again, the mineral surfaces appear to be coated.



**This Page is Inserted by IFW Indexing and Scanning
Operations and is not part of the Official Record**

BEST AVAILABLE IMAGES

Defective images within this document are accurate representations of the original documents submitted by the applicant.

Defects in the images include but are not limited to the items checked:

- ☐ BLACK BORDERS
- ☐ IMAGE CUT OFF AT TOP, BOTTOM OR SIDES
- ☐ FADED TEXT OR DRAWING
- ☐ BLURRED OR ILLEGIBLE TEXT OR DRAWING
- ☐ SKEWED/SLANTED IMAGES
- ☐ COLOR OR BLACK AND WHITE PHOTOGRAPHS
- ☐ GRAY SCALE DOCUMENTS
- ☒ LINES OR MARKS ON ORIGINAL DOCUMENT
- ☐ REFERENCE(S) OR EXHIBIT(S) SUBMITTED ARE POOR QUALITY
- ☐ OTHER: _____

IMAGES ARE BEST AVAILABLE COPY.

As rescanning these documents will not correct the image problems checked, please do not report these problems to the IFW Image Problem Mailbox.